



### **Science Arts & Métiers (SAM)**

is an open access repository that collects the work of Arts et Métiers Institute of Technology researchers and makes it freely available over the web where possible.

This is an author-deposited version published in: <https://sam.ensam.eu>  
Handle ID: [.http://hdl.handle.net/10985/22116](http://hdl.handle.net/10985/22116)

#### **To cite this version :**

Nolwenn FOUGERON, Pierre-Yves ROHAN, Jean-Loïc ROSE, Xavier BONNET, Helene PILLET  
- Finite element analysis of the stump-ischial containment socket interaction: a technical note -  
Medical Engineering & Physics - Vol. 105, p.103829 - 2022

Any correspondence concerning this service should be sent to the repository

Administrator : [scienceouverte@ensam.eu](mailto:scienceouverte@ensam.eu)



1 **Impact of the ischial support in ischial**  
2 **containment socket on the stump-socket**  
3 **interaction: a finite element study**

4 **Nolwenn Fougeron<sup>1,2</sup>, Pierre-Yves Rohan<sup>1</sup>, Jean-Loïc Rose<sup>2</sup>, Xavier Bonnet<sup>1</sup>,**  
5 **Hélène Pillet<sup>1</sup>**

6 <sup>1</sup> Institut de Biomécanique Humaine Georges Charpak, Arts et Métiers ParisTech, 151 bd de l'Hôpital, 75013.  
7 Paris, France

8 <sup>2</sup> Proteor, Recherche et développement, 5 boulevard Winston Churchill, 21000 Dijon, France

9 Corresponding author:

10 **Hélène Pillet**

11 **LBM/Institut de Biomécanique Humaine Georges Charpak**

12 **Arts et Métiers ParisTech**

13 **151 bd de l'Hôpital 75013 Paris**

14 E-mail: [helene.pillet@ensam.eu](mailto:helene.pillet@ensam.eu)

15 Keywords (max 6): Above-knee amputee; Prosthetic socket; Finite Element Modeling; Musculoskeletal modeling;

16 Pressure

17 Word count: 3 499

## 18 Abstract

19 The role of the above-knee socket is to ensure the load transfer via the coupling of residual limb-  
20 prosthesis with minimal discomfort and without damaging the soft tissues. Modelling is a potential tool to  
21 predict socket fit prior to manufacture. However, state-of-the-art models only include the femur in soft tissues  
22 submitted to static loads neglecting the contribution of the hip joint. The hip joint is particularly challenging to  
23 model because it requires to compute the forces of muscles inserting on the residual limb. This work proposes a  
24 modelling of the hip joint including the estimation of muscular forces using a combined MusculoSkeletal  
25 (MSK)/Finite Element (FE) framework. An experimental-numerical approach was conducted on one femoral  
26 amputee subject. This allowed to i) model the hip joint and personalize muscles forces, ii) study the impact of the  
27 ischial support, and iii) evaluate the interface pressure. A reduction of the gluteus medius force from the MSK  
28 modelling was noticed when considering the ischial support. Interface pressure, predicted between 63 to 71 kPa,  
29 agreed with experimental literature data. The contribution of the hip joint is a key element of the modelling  
30 approach for the prediction of the socket interface pressure with the residual limb soft tissues.

31 *Word count: 200*

32

33

# Introduction

34 Advances in modelling of soft tissues have led to a better understanding of the mechanical loads  
35 transmission during the interaction with prosthetic devices and their consequences for tissue viability and  
36 integrity. FE models of below-knee amputations have been proposed by several research groups for the  
37 estimation of interface pressures prior to the socket fabrication in order to evaluate and modify, if needed, the  
38 socket shape [1]–[3]. Concerning above-knee amputations fewer attempts have been proposed [4]. Most residual  
39 limb models only include the femur in soft tissues, with generic mechanical properties, submitted to static loads  
40 that are poorly representatives of the loads imposed during gait. A consequence is that confidence in model  
41 predictions has not been established in the literature. Only two studies have focused on the experimental  
42 verification of above-knee amputation models but without satisfying results in terms prediction accuracy and  
43 systematic experimental validation [5], [6].

44 The difficulties to validate FE models may be explained by the absence of the pelvis, and particularly of  
45 the ischium, in the model. Yet, the ischium is the weightbearing area of the socket and is a significant pivot point  
46 affecting the person balance and the transmission of loads as highlighted by experimental pressure measurements  
47 [7]–[11].

48 Amongst the above-knee residual limb FE models [5], [6], [20]–[23], [12]–[19], only one [20] explicitly  
49 represented the pelvis. The bony structure consisted of the residual femur and the ischium fused together.  
50 Contrary to models that considered only the femur, this last model predicted peak pressure located under the  
51 ischium, in agreement with experimental observations [9]–[11]. Nevertheless, the magnitude of the peak  
52 pressure, 364 kPa, was higher than those of experimental measurements that are reported to be lower than 300  
53 kPa [10]. This overestimation may be due to the fusion of the bones which do not account for the relative  
54 movement of the femur and pelvis. However, a realistic modelling of this movement not only necessitate to  
55 allow rotational degrees of freedom of the hip joint in the FE model but also to properly define the distribution of  
56 the mechanical loads at the hip joint level.

57 The computation of the loads distribution during the stance phase is challenging. Considering the  
58 mechanical equilibrium in a section passing through the hip, the loads expressed at the hip centre are obtained by  
59 summing the external loads applied to the pelvis segment (Figure 1). The external forces to consider are  
60 muscular forces ( $T_{\text{muscles}}$ ), contact force of the residual femur ( $F_{\text{femur}}$ ), ligaments' forces that can be neglected,  
61 [24], the action of the trunk, the contralateral limb and the weight of the subject minus the weight of the residual

62 limb ( $W$ ) and the contact force with soft tissues which could actually be divided in two: the contact force due to  
63 the ischial support ( $F_{\text{ischial support}}$ ), and the contact force due to the tightening of the socket all over the residual  
64 limb ( $F_{\text{contact}}$ ). A correct estimation of the hip behaviour in the FE model impose to quantify muscular forces  
65 during gait, using MSK modelling for example.

66 **FIGURE 1**

67 However, MSK models of amputee subjects neglect the contribution of the contact force on the ischial  
68 support [25]–[29] which goes against the mechanical model described by [30]. Indeed, this force is supposed to  
69 be equivalent to at least 50 % of the person weight and thus to induce a non-negligible moment at the hip centre  
70 in the frontal plane. Yet, few data are available on the contribution of the ischial support on the distribution of  
71 the mechanical loads.

72 The methodology for introducing a more realistic modelling of the hip joint included the estimation of  
73 muscular forces using a MSK model of the hip joint combined with a FE framework to consider the interaction  
74 with a prosthesis. The current study focused in the frontal plane as it is the most impacted component of the net  
75 hip moment due to the ischial support. The contact loads applied by the ischial support varied to quantify the  
76 impact of the ischial support on muscular forces, with the MSK model, and on the pressure distribution at the  
77 interface with the socket, with the FE framework.

78

# Materials and methods

## 79 2.1. Experimental acquisitions

80 One volunteer wearing an ischial containment socket participated to the study after informed consent  
81 and approval of the *Comité de Protection des Personnes* (CPP NX06036). The volunteer was 54 years old,  
82 amputated 7 years ago and had a daily usage of his/her prosthesis.

### 83 2.1.1. Movement analysis

84 Motion capture acquisitions were carried out with a Vicon optoelectronic system (Vicon, Oxford  
85 Metrics Ltd, Oxford, UK) with thirteen cameras and four AMTI force plates (AMTI Advanced Mechanical  
86 Technology, Inc, Massachusetts, OR6-5). The volunteer was equipped with 55 optoelectronic markers on the  
87 lower limbs following the protocol of [31].

88 The subject was instructed to walk in a straight line, along which the force plates were positioned, on a  
89 flat floor at a self-selected speed. The acquisitions stopped once five complete walk cycles were recorded.

### 90 2.1.2. Imaging

91 A pair of EOS radiographs (EOS Imaging, Paris, France) was acquired in the standard standing posture  
92 [32], after the motion capture acquisitions, with markers in place. Subject-specific 3D reconstructions of the  
93 pelvis and femur were performed from the EOS radiographs according to procedures developed previously [32],  
94 [33] and based on the work of [34] (Figure 2). The geometry of the intact femur was replicated and symmetrized  
95 to define the geometry of the residual femur. The position of this femur was manually adjusted using the  
96 radiographs and cut at the level of the amputation.

97 FIGURE 2

98 The prosthetist of the volunteer provided the rectified plaster used to design the socket. This plaster was  
99 scanned using a 3D optical scanner (EinScan-Pro, Shining 3D, USA) to reconstruct the internal shape of the  
100 socket and the external envelop of the soft tissues.

## 101 2.2. FE modelling

### 102 2.2.1. Model geometry

103 The FE model was designed to predict pressures at the surface of the residual limb at 25 % of the gait  
104 cycle, which corresponds to a single leg stance. The geometry included the residual femur, pelvis, soft tissues  
105 and socket (Figure 3). Muscles acting on the hip degrees of freedom were defined according to literature data

106 [35] and modelled as linear springs. Insertions were personalized thanks to a kriging method with control points  
107 defined from the bones 3D reconstructions, like for the musculoskeletal model described below.

108 The pelvis geometry was simplified to include only the acetabulum, ischium and pubis. The pelvis was  
109 rotated around the femoral head centre so that its relative position with the residual femur was the one computed  
110 at 25 % of the gait cycle. The liner and the soft tissues were fused together. The geometry of the socket was also  
111 used to define the external envelop of the soft tissues. The initial tightening of the socket was modelled with a  
112 uniform radial reduction of its volume by 2 % following the advices of prosthetists. The joint capsule around the  
113 hip joint was model by subtracting the volume of soft tissues contained in a sphere centred on the femoral head  
114 with a radius equals to 150 % of the femoral head radius. The volumes of soft tissues and socket were meshed  
115 with hybrid linear tetrahedral elements (C3D4H). A total of 86 539 elements were defined. The mesh size was  
116 set according the mesh convergence analysis of the interface peak pressure.

### 117 2.2.2. *Material properties*

118 The socket consisted of a distal and mid wall and a proximal edge. Both parts were modelled with a first  
119 order Ogden hyperelastic isotropic homogenous constitutive law [3]. A shear modulus of 121 MPa was assigned  
120 to the distal part of the socket, while the proximal shear modulus was fixed to 60.5 MPa. The material parameter  
121  $\alpha$  and the Poisson coefficient were set to 2 and 0.49 respectively [3]. Soft tissues volumes were also modelled  
122 with a first order Ogden hyperelastic law. Personalized constitutive parameters were estimated using an original  
123 protocol combining freehand ultrasound-based indentations and inverse FE modelling previously reported by  
124 [36]. The shear modulus was evaluated to 12.1 kPa and the material parameter  $\alpha$  to 11. The Poisson coefficient  
125 was assumed to be equal to 0.45 to model a quasi-incompressible behaviour but also to facilitate the convergence  
126 of the analysis. Bones were assumed rigid.

### 127 2.2.3. *Interactions and contact hypothesis*

128 The connection between the residual femur and the pelvis bone was modelled with a universal joint.  
129 Only the external/internal rotation degree of freedom was blocked in this first approach. The contact between  
130 soft tissues and bones was modelled with a tie constraint. A friction contact was assumed between the socket and  
131 the liner/soft tissue surface with the coefficient of friction set according to the analysis step.

## 132 2.3. FE Analysis

### 133 2.3.1. *Initial step: donning of the socket*

134 The initial step was performed to pre-stress the soft tissues with the donning of the socket. A vertical  
135 displacement of 130 mm was imposed to the pelvis, whilst socket degrees of freedom were blocked. The

136 displacement was such that the relative position of the residual femur and the socket corresponded to that  
137 computed from the inverse kinematic at the defined gait cycle time step. Muscles stiffnesses were estimated  
138 proportionally to their physical cross-sectional areas, in order to stabilise the femur during the pelvis  
139 displacement. The FE analysis was performed with an implicit scheme. During this step, the coefficient of  
140 friction between the socket and the liner/soft tissues surface was set to 0.3 [37].

### 141 2.3.2. Final step: walking loads

142 A final step was set to apply walking loads at the knee centre as a boundary condition. The coefficient of  
143 friction between the socket and the liner/soft tissues surfaces was set to 1 to limit the relative sliding at this  
144 interface. As first approximation, in order to investigate the contribution of the ischial support in the frontal  
145 plane, only loads that resulted in an abduction/adduction moment at the hip centre were applied to the socket  
146 (Table 1). The position of the pelvis was fixed during this step.

147 A MSK model of the hip joint, developed in the next section, was designed in order to compute the muscular  
148 forces (Figure 3) to input in the FE model at 25 % of the gait cycle. These forces were applied to the linear  
149 springs used to model each muscle.

## 150 2.4. MSK modelling

### 151 2.4.1. Muscular forces computation

152 The MSK model was designed from the bones reconstructions to estimate the muscles forces designed  
153 with MATLAB (The MathWorks, Inc., Matlab) using literature models [35]. The kinematics of the femur and  
154 the pelvis were inferred from the motion capture data [38]. The net joint loads and the external loads applied to  
155 the system were computed from an inverse dynamic analysis. A static optimization was used to assess the  
156 muscular forces (Figure 3).

157 To account for the amputation of the femur, only muscles acting on the hip mobility were preserved.  
158 Remaining muscles insertions and path points were personalized with a kriging method [39] using the 3D bones  
159 reconstructions. Insertion points below the level of amputation were fixed to the distal end of the residual femur.  
160 Eventually, the model was composed of the residual femur, the pelvis and the following muscles: adductor  
161 magnus, long head of the biceps femoris, gemini muscles, gluteus maximus (in three portions), gluteus medius  
162 (in three portions), gracilis, iliac, pectineus, piriformis, psoas, quadratus femoris, rectus femoris, sartorius, and  
163 tensor fasciae latae (Figure 3).

164 The net hip forces and moments are distributed between muscular, ligament and contact forces.  
165 Ligaments 'forces were neglected here. It was also assumed that the femur contact force did not induce any hip

166 moment at the joint centre. The remaining forces were the muscle forces and the soft tissue contact force that  
 167 was supposed to be mainly located under the ischium.

168 To solve the system, the method developed by [24] was adapted to the amputated gait. As hypothesized  
 169 by [30], at least 50 % of the body weight is applied on the ischial support of the socket. Without further  
 170 information, it was speculated that the moment of the contact force at the ischium reduced the net abduction  
 171 moment by 50 %.

172 All these hypotheses led to the following system of equations:

173 (1) 
$$J(x) = \sum_{i=1}^n \left( \frac{F_i}{F_i^{max}} \right)^2$$

174 (2) 
$$\begin{cases} \begin{pmatrix} r_{abd1} & \dots & r_{abdn} \\ r_{rot1} & \dots & r_{rotn} \\ r_{flex1} & \dots & r_{flexn} \end{pmatrix} \times x = \begin{bmatrix} 0.5 * M_{abd} \\ M_{rot} \\ M_{flex} \end{bmatrix}, \\ 0 \leq x \leq F^{max} \end{cases}$$

175 With J, the cost function to minimize,  $F^i$  the force of the  $i^{th}$  muscle,  $F_{max}^i$  the maximal isometric force of  
 176 the  $i^{th}$  muscle from literature data [35],  $x$  a n-by-1 vector of all muscular forces,  $F_{max}$  the n-by-1 vector of  
 177 maximal isometric forces. The kinematic analysis and the 3D models of the bones were used to compute  $r_{abd}^i$ ,  $r_{rot}^i$   
 178 and  $r_{flex}^i$ , the lever arms of the  $i^{th}$  muscle with the hip centre respectively in abduction/adduction, internal/external  
 179 rotation and flexion/extension [40].  $M_{abd}$ ,  $M_{rot}$  and  $M_{flex}$ , the net hip moment components respectively in  
 180 abduction/adduction, internal/external rotation and flexion/extension from the inverse dynamic analysis,  $n$  the  
 181 total number of muscles [35].

182 The muscular forces were comprised between zero to  $F_{max}$ . As a first approach, the internal/external rotation  
 183 moment was set to zero, as this value was negligible compared with the other components (

184 ). The optimization was performed using the *fmincon* built-in MATLAB function. Values obtained for  $x$   
 185 were extracted at 25 % of the gait cycle and added as nodal forces in the FE model.

#### 186 2.4.2. Hip abduction moment reduction

187 No data on the reduction of the net hip abduction moment due to the use of a prosthetic socket were  
 188 available. Therefore, three conditions were studied with a reduction by 0%, 50% and 100% [30], 0 % reduction  
 189 meaning there was no weight applied to the ischial support of the socket whereas 100 % reduction meaning that  
 190 all of the weight was on the ischial support. A control model, with no degrees of freedom for the hip joint and no  
 191 muscular forces, was also computed to emphasize the usefulness of the modelling of this joint.

192 FIGURE 3



# Results

194

## 3.1. Joint loads and muscles forces

195

196 Loads at the knee and hip centre computed from the inverse dynamics at 25 % of the gait cycle are  
197 summarized in

198 . Loads expressed at the knee joint centre are expressed in the femur reference frame [41] and loads  
199 expressed at the hip joint centre are expressed in the pelvis reference frame [42].

200 TABLE 1

201 Gluteus medius forces are presented for the entire gait cycle in Figure 4 for a net hip moment reduction  
202 of 0 %, 50 % and 100 %. In terms of intensity, the gluteus medius developed the major force during the entire  
203 stance phase and the impact of the ischial support is particularly clear on this muscle, for which the more support  
204 the less muscle activation.

205 FIGURE 4

## 3.2. FE-MSK analyses

206

207 Simulations lasted less than 40 minutes using two CPU cores. The computer used had an Intel® Xeon®  
208 E-2174G CPU @3.80 GHz and 16 GB RAM. The peak pressure was always located under the ischium in the  
209 region of the ischial support no matter the net hip moment reduction (Figure 4). Peak pressures were very similar  
210 from one model to another with the hip joint and were up to 71 kPa for 0 % reduction, 63 kPa for 50 % reduction  
211 and 67 kPa for 100 % reduction. Pressure maps varied slightly on the other areas of the residual limb among the  
212 three models. On the contrary, the pressure distribution changed for the model with no degrees of freedom at the  
213 hip joint. Peak pressure was up to 127 kPa for this model.

214 FIGURE 5

## Discussion

215  
216  
217  
218  
219  
220  
221  
222  
223  
224  
225  
226  
227  
228  
229  
230  
231  
232  
233  
234  
235  
236  
237  
238  
239  
240  
241  
242

The objective was to develop a new model of the interaction of the above-knee residual limb and the socket by combining FE and MSK modelling, using MSK data to model muscular forces in the FE model. This is also the first approach for the evaluation of pressure distribution at the interface with the socket that integrated a realistic modelling of the hip joint. To do so, FE and MSK models were used to assess the distribution of the mechanical loads at the hip centre which allowed to account for the interaction with prosthesis during gait as highlighted by [30].

In this contribution, a subject-specific MSK model of the hip joint that accounts for the interplay between the ischiatic support and the pelvis has been combined with the FE framework. In fact, the estimation of the muscular forces during amputated gait has received little attention. Moreover, existing studies were based on methods developed for the asymptomatic gait [26]–[29], neglecting the interaction with the socket. In this work, the prosthesis was accounted by a reduction of the net hip abduction moment, as suggested by [30]. This mainly resulted in a reduction of the force developed by the main hip abductor muscle, the gluteus medius. These estimated muscular forces were implemented in the FE model. Peak pressures were 71 kPa, 63 kPa and 67 kPa, respectively for a reduction of the net hip moment by 0 %, 50 % and 100 %. Differences between models were mainly localized under the ischium but were at most 8 kPa. The differences estimated here were small compared to the differences in muscular forces. These small changes may be explained by the simplification of the muscles modelling. A volumetric representation of the muscles as proposed by [43] may provide better insights into the impact of the muscular activation on the interface pressure. However, the modelling of the free hip joint did allow i) to estimate correct pressure distribution with the peak pressure located at the ischial support level as expected, and ii) to respect the load distributions as described by [30]. In fact, another study presented a FE model of a residual limb with and without the hip joint [20]. The authors highlighted the importance to model the hip joint to estimate proper pressure distribution. To go further, the modelling of the hip joint has to consider the muscular forces to avoid overestimation of pressure distribution as emphasized by the present results.

Few experimental studies reported measurements performed during walking activities with sensors positioned all over the residual limb [7]–[11]. Among these studies peak pressure was always located under the ischium with maxima between 30 kPa [7] and 300 kPa [10] which is in accordance with the FE model presented in this study.

243 Simplifications may have a negative impact on the accuracy of the pressure estimations. First, pre-stress  
244 of the soft tissues due to the socket tightening was performed by radially reducing the socket volume. While this  
245 configuration did not account for the actual initial stress state the impact had probably a negligible impact on the  
246 final pressure values since pressure reported during the donning phase are much lower than those reported for  
247 standing or walking activities [17], [20]. Other hypothesis may have a small or negligible impact such as the  
248 simplification of the residual femur geometry obtained from the contralateral femur. On the other hand, the  
249 impact of the value of the coefficient of friction with the socket also need to be studied since this parameter was  
250 set arbitrarily in this paper. The fusion of the soft tissues and the liner may have influenced the results since this  
251 modelling approach did not allow to account for the material properties of the different components. The whole  
252 residual limb was also modelled with a single pair of parameters even though material parameters differs  
253 according to body areas and may have a significant impact on the mechanical response of the model [44]. Small  
254 errors of pressure values may also exist due to the use of linear tetrahedral elements. With regard to the MSK  
255 model, muscles' parameters, except geometry, were extracted from the literature [35]. The amputation technique  
256 was also shown to impact the estimation of muscular forces [27], but in this approach, all muscles inserted lower  
257 than the amputation level were attached to the residual femur distal end.

258 This model still needs to be validated. To do so, an experimental campaign with pressure measurements  
259 at the interface with the socket has to be conducted.

260

261

## Conclusion

262

A combined FE and MSK modelling approach was proposed in this contribution to evaluate the

263

pressure at the interface between a prosthetic socket and the residual limb. In this context, numerical modelling

264

paves the way for innovative socket design process. By combining the experience and the knowledge of the

265

prosthetists and the robustness of numerical analysis, socket design could require less iterations to provide more

266

comfortable sockets and, on top of that, could help to conceive sockets for patients who present particular

267

difficulties in fitting, such as poor bone relief, or are unable to provide their prosthetist with feedback. Even

268

though modelling processes still require cumbersome imaging and computation tools, some approaches detailed

269

in the literature describe methods for the spreading of FE analyses in the clinical routine [1], [2], [45], [46] that

270

back up the relevance of such approaches in the orthopaedic field. Yet, experimental validation evidence of

271

digital twins must be obtained prior to any clinical evaluation and relies on the capacity to assess experimental

272

data in the clinical environment.

273

274

## Acknowledgement

275 The authors are also grateful to the ParisTech BiomecAM chair program on subject-specific  
276 musculoskeletal modeling (with the support of ParisTech and Yves Cotrel Foundations, Société Générale, Proteor  
277 and Covea) and to Proteor for their financial support.

278

## Conflict of interest

279 The authors certify that no conflict of interest is raised by this work.

280

281

## Ethical Approval

282 This study was approved by the *Comité de Protection des Personnes* (CPP NX06036).

283

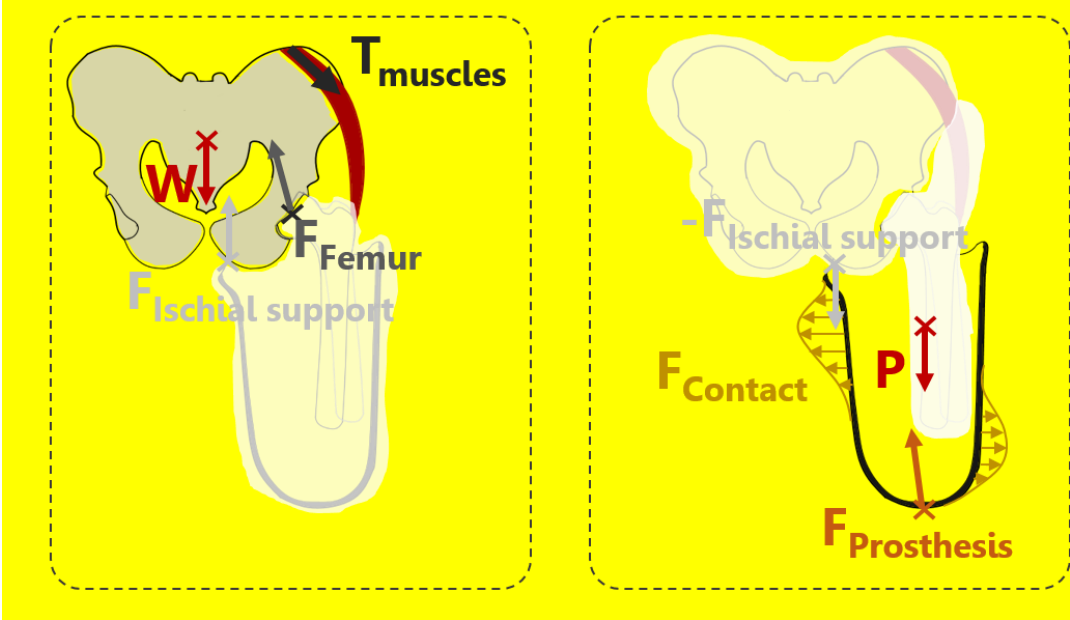
## References

- 284 [1] J. W. Steer, P. A. Grudniewski, M. Browne, P. R. Worsley, A. J. Sobey, and A. S. Dickinson,  
285 “Predictive prosthetic socket design: part 2—generating person-specific candidate designs using multi-  
286 objective genetic algorithms,” *Biomech. Model. Mechanobiol.*, 2019, doi: 10.1007/s10237-019-01258-7.
- 287 [2] J. W. Steer, P. R. Worsley, M. Browne, and A. S. Dickinson, “Predictive prosthetic socket design: part  
288 1—population-based evaluation of transtibial prosthetic sockets by FEA-driven surrogate modelling,”  
289 *Biomech. Model. Mechanobiol.*, no. 0123456789, 2019, doi: 10.1007/s10237-019-01195-5.
- 290 [3] K. M. Moerman, D. M. Sengh, and H. M. Herr, “Automated and Data-driven Computational Design of  
291 Patient-Specific Biomechanical Interfaces,” *IEEE Access*, 2016, doi:  
292 <https://doi.org/10.31224/osf.io/g8h9n>.
- 293 [4] A. S. Dickinson, J. W. Steer, and P. R. Worsley, “Finite element analysis of the amputated lower limb: A  
294 systematic review and recommendations,” *Medical Engineering and Physics*. 2017, doi:  
295 10.1016/j.medengphy.2017.02.008.
- 296 [5] G. Colombo, C. Comotti, D. F. Redaelli, D. Regazzoni, C. Rizzi, and A. Vitali, “A method to improve  
297 prosthesis leg design based on pressure analysis at the socket-residual limb interface,” *Proc. ASME Des.*  
298 *Eng. Tech. Conf.*, vol. 1A-2016, pp. 1–8, 2016, doi: 10.1115/DETC2016-60131.
- 299 [6] M. S. Jamaludin, A. Hanafusa, Y. Shinichirou, Y. Agarie, H. Otsuka, and K. Ohnishi, “Analysis of  
300 pressure distribution in transfemoral prosthetic socket for prefabrication evaluation via the finite element  
301 method,” *Bioengineering*, vol. 6, no. 4, 2019, doi: 10.3390/bioengineering6040098.
- 302 [7] P. V. S. Lee, S. E. Solomonidis, and W. D. Spence, “Stump-socket interface pressure as an aid to socket  
303 design in prostheses for trans-femoral amputees—a preliminary study,” *Proc. Inst. Mech. Eng. Part H J.*  
304 *Eng. Med.*, vol. 211, no. 2, pp. 167–180, 1997, doi: 10.1243/0954411971534287.
- 305 [8] F. A. Appoldt and L. Bennett, “A preliminary report on dynamic socket pressures,” *Bull. Prosthet. Res.*,  
306 vol. 10, no. 8, pp. 20–55, 1967.
- 307 [9] F. Appoldt, L. Bennett, and R. Contini, “Stump-socket pressure in lower extremity prostheses,” *J.*  
308 *Biomech.*, vol. 1, no. 4, pp. 247–257, 1968, doi: 10.1016/0021-9290(68)90020-1.
- 309 [10] B. Moineau, “Analyses des pression a l’interface moignon-emboiture de la prothèse chez le patient  
310 amputé fémoral,” 2017.
- 311 [11] J. T. Kahle and M. J. Highsmith, “Transfemoral sockets with vacuum-assisted suspension comparison of  
312 hip kinematics, socket position, contact pressure, and preference: Ischial containment versus brimless,”  
313 *J. Rehabil. Res. Dev.*, vol. 50, no. 9, pp. 1241–1252, 2014, doi: 10.1682/jrrd.2013.01.0003.
- 314 [12] M. Malinauskas, T. A. Krouskop, and P. A. Barry, “Noninvasive measurement of the stiffness of tissue  
315 in the above-knee amputation limb,” *J. Rehabil. Res. Dev.*, vol. 26, no. 3, pp. 45–52, 1989.

- 316 [13] M. Zhang and A. F. T. Mak, "A finite element analysis of the load transfer between an above-knee  
317 residual limb and its prosthetic socket - Roles of interface friction and distal-end boundary conditions,"  
318 *IEEE Trans. Rehabil. Eng.*, vol. 4, no. 4, pp. 337–346, 1996, doi: 10.1109/86.547935.
- 319 [14] F. von Waldenfels, S. Raith, M. Eder, A. Volf, J. Jalali, and L. Kovacs, "Computer Assisted  
320 Optimization of Prosthetic Socket Design for the Lower Limb Amputees Using 3-D Scan," no. October,  
321 pp. 15–20, 2012, doi: 10.15221/12.015.
- 322 [15] L. Kovacs *et al.*, "Patient- Specific Optimization of Prosthetic Socket Con- struction and Fabrication  
323 Using Innovative Manufacturing Processes: A Project in Progress," *Proc. Mater. World Conf. 2010*,  
324 2010.
- 325 [16] L. Zhang, M. Zhu, L. Shen, and F. Zheng, "Finite element analysis of the contact interface between  
326 trans-femoral stump and prosthetic socket," in *Proceedings of the Annual International Conference of*  
327 *the IEEE Engineering in Medicine and Biology Society, EMBS*, 2013, pp. 1270–1273, doi:  
328 10.1109/EMBC.2013.6609739.
- 329 [17] S. C. Henao, C. Orozco, and J. Ramírez, "Influence of Gait Cycle Loads on Stress Distribution at The  
330 Residual Limb/Socket Interface of Transfemoral Amputees: A Finite Element Analysis," *Sci. Rep.*, vol.  
331 10, no. 1, pp. 1–11, 2020, doi: 10.1038/s41598-020-61915-1.
- 332 [18] V. Restrepo, J. Villarraga, and J. P. Palacio, "Stress reduction in the residual limb of a transfemoral  
333 amputee varying the coefficient of friction," *J. Prosthetics Orthot.*, vol. 26, no. 4, pp. 205–211, 2014,  
334 doi: 10.1097/JPO.0000000000000044.
- 335 [19] R. Surapureddy, S. Stagon, A. Schönning, and A. Kassab, "Predicting pressure distribution between  
336 transfemoral prosthetic socket and residual limb using finite element analysis," *Int. J. Exp. Comput.*  
337 *Biomech.*, vol. 4, no. 1, p. 32, 2016, doi: 10.1504/ijecb.2016.10002681.
- 338 [20] A. Van Heesewijk, A. Crocombe, S. Cirovic, M. Taylor, and W. Xu, "Evaluating the Effect of Changes  
339 in Bone Geometry on the Trans-femoral Socket-Residual Limb Interface Using Finite Element  
340 Analysis," in *World Congress on Medical Physics and Biomedical Engineering*, 2018, pp. 367–370, doi:  
341 10.1007/978-981-10-9038-7.
- 342 [21] E. Ramasamy *et al.*, "An Efficient Modelling-Simulation-Analysis Workflow to Investigate Stump-  
343 Socket Interaction Using Patient-Specific, Three-Dimensional, Continuum-Mechanical, Finite Element  
344 Residual Limb Models," *Front. Bioeng. Biotechnol.*, vol. 6, no. September, pp. 1–17, 2018, doi:  
345 10.3389/fbioe.2018.00126.
- 346 [22] A. J. Sanchez-Alvarado, V. Nováček, and J. Křen, "A framework to assess mechanics of stump–socket  
347 interaction in transfemoral amputees," *Lek. a Tech.*, vol. 49, no. 2, pp. 46–51, 2019, doi:  
348 10.14311/CTJ.2019.2.02.
- 349 [23] Z. Meng, D. W. C. Wong, M. Zhang, and A. K. L. Leung, "Analysis of compression/release stabilized  
350 transfemoral prosthetic socket by finite element modelling method," *Med. Eng. Phys.*, vol. 83, pp. 123–  
351 129, 2020, doi: 10.1016/j.medengphy.2020.05.007.
- 352 [24] R. D. Crowninshield and R. A. Brand, "The prediction of forces in joint structures: Distribution of  
353 intersegmental resultants," *Exercise and Sport Sciences Reviews*, vol. 9, no. 1. pp. 159–181, 1981, doi:  
354 10.1249/00003677-198101000-00004.
- 355 [25] T. S. Bae, K. Choi, D. Hong, and M. Mun, "Dynamic analysis of above-knee amputee gait," *Clin.*  
356 *Biomech.*, vol. 22, no. 5, pp. 557–566, 2007, doi: 10.1016/j.clinbiomech.2006.12.009.
- 357 [26] Y. Suzuki, "Dynamic optimization of transfemoral prosthesis during swing phase with residual limb  
358 model," *Prosthet. Orthot. Int.*, vol. 34, no. 4, pp. 428–438, 2010, doi: 10.3109/03093646.2010.484829.
- 359 [27] E. C. Ranz, J. M. Wilken, D. A. Gajewski, and R. R. Neptune, "The influence of limb alignment and  
360 transfemoral amputation technique on muscle capacity during gait," *Comput. Methods Biomech. Biomed.*  
361 *Engin.*, vol. 20, no. 11, pp. 1167–1174, 2017, doi: 10.1080/10255842.2017.1340461.
- 362 [28] A. Mohamed, "Modeling and Simulation of Transfemoral Amputee Gait," University of New  
363 Brunswick, 2018.
- 364 [29] V. J. Harandi *et al.*, "Gait compensatory mechanisms in unilateral transfemoral amputees," *Med. Eng.*  
365 *Phys.*, vol. 77, pp. 95–106, 2020, doi: 10.1016/j.medengphy.2019.11.006.
- 366 [30] C. W. Radcliffe, "Functional considerations in the fitting of above-knee prostheses.," *Artif. Limbs*, vol. 2,  
367 no. 1, pp. 35–60, 1955, doi: 10.1017/CBO9781107415324.004.
- 368 [31] H. Goujon-Pillet, E. Sapin, P. Fodé, and F. Lavaste, "Three-Dimensional Motions of Trunk and Pelvis  
369 During Transfemoral Amputee Gait," *Arch. Phys. Med. Rehabil.*, vol. 89, no. 1, pp. 87–94, 2008, doi:  
370 10.1016/j.apmr.2007.08.136.
- 371 [32] Y. Chaibi *et al.*, "Fast 3D reconstruction of the lower limb using a parametric model and statistical  
372 inferences and clinical measurements calculation from biplanar X-rays," *Comput. Methods Biomech.*  
373 *Biomed. Engin.*, vol. 15, no. 5, pp. 457–466, 2012, doi: 10.1080/10255842.2010.540758.
- 374 [33] D. Mitton *et al.*, "3D reconstruction of the pelvis from bi-planar radiography," *Comput. Methods*  
375 *Biomech. Biomed. Engin.*, vol. 9, no. 1, pp. 1–5, 2006, doi: 10.1080/10255840500521786.

- 376 [34] J. Dubousset, G. Charpak, W. Skalli, J. Deguise, and G. Kalifa, "EOS: A NEW IMAGING SYSTEM  
377 WITH LOW DOSE RADIATION IN STANDING POSITION FOR SPINE AND BONE & JOINT  
378 DISORDERS," *J. Musculoskelet. Res.*, vol. 13, no. 01, pp. 1–12, 2010, doi:  
379 10.1142/S0218957710002430.
- 380 [35] A. Seth *et al.*, "OpenSim: Simulating musculoskeletal dynamics and neuromuscular control to study  
381 human and animal movement," *PLoS Comput. Biol.*, vol. 14, no. 7, p. e1006223, 2018, doi:  
382 10.1371/journal.pcbi.1006223.
- 383 [36] N. Fougerson, P.-Y. Rohan, D. Haering, J.-L. Rose, X. Bonnet, and H. Pillet, "Combining Freehand  
384 Ultrasound-Based Indentation and Inverse Finite Element Modeling for the Identification of Hyperelastic  
385 Material Properties of Thigh Soft Tissues," *J. Biomech. Eng.*, vol. 142, no. 9, 2020, doi:  
386 10.1115/1.4046444.
- 387 [37] M. Zhang, A. R. Turner-Smith, V. C. Roberts, and A. Tanner, "Frictional action at lower limb/prosthetic  
388 socket interface," *Med. Eng. Phys.*, vol. 18, no. 3, pp. 207–214, 1996, doi: 10.1016/1350-  
389 4533(95)00038-0.
- 390 [38] B. Panhelleux, N. Fougerson, N. Ruysen, P.-Y. Rohan, X. Bonnet, and H. Pillet, "Femoral  
391 residuum/socket kinematics using fusion between 3D motion capture and stereo radiography," *Comput.  
392 Methods Biomech. Biomed. Engin.*, vol. 22, no. sup1, pp. S245–S247, 2019, doi:  
393 10.1080/10255842.2020.1714257.
- 394 [39] F. Trochu, "A contouring program based on dual kriging interpolation," *Eng. Comput.*, vol. 9, no. 3, pp.  
395 160–177, 1993, doi: 10.1007/BF01206346.
- 396 [40] F. E. Zajac and M. E. Gordon, "Determining Muscle's Force and Action in Multi-Articular Movement,"  
397 *Exerc. Sport Sci. Rev.*, vol. 17, no. 1, pp. 187–230, 1989.
- 398 [41] a Cappozzo, F. Catani, U. Della Croce, and a Leardini, "Position and orientation in space of bones  
399 during movement," *Clin. Biomech.*, vol. 10, no. 4, pp. 171–178, 1995, [Online]. Available: pdf AHa.
- 400 [42] R. Dumas, T. Robert, L. Cheze, and J. P. Verriest, "Thorax and abdomen body segment inertial  
401 parameters adjusted from McConville *et al.* and Young *et al.*," *Int. Biomech.*, vol. 2, no. 1, pp. 113–118,  
402 2015, doi: 10.1080/23335432.2015.1112244.
- 403 [43] J. Stelletta, R. Dumas, and Y. Lafon, "Modeling of the Thigh: A 3D Deformable Approach Considering  
404 Muscle Interactions," *Biomech. Living Organs Hyperelastic Const. Laws Finite Elem. Model.*, pp. 497–  
405 521, 2017, doi: 10.1016/B978-0-12-804009-6.00023-7.
- 406 [44] A. Macron *et al.*, "Is a simplified Finite Element model of the gluteus region able to capture the  
407 mechanical response of the internal soft tissues under compression?," *J. Tissue Viability*, vol. 217, pp.  
408 81–90, 2019.
- 409 [45] B. J. Ranger, M. Feigin, X. Zhang, K. M. Moerman, H. Herr, and B. W. Anthony, "3D ultrasound  
410 imaging of residual limbs with camera-based motion compensation," *IEEE Trans. Neural Syst. Rehabil.  
411 Eng.*, vol. 27, no. 2, pp. 207–217, 2019, doi: 10.1109/TNSRE.2019.2894159.
- 412 [46] D. Solav, K. M. Moerman, A. M. Jaeger, and H. M. Herr, "A Framework for Measuring the Time-  
413 Varying Shape and Full-Field Deformation of Residual Limbs Using 3-D Digital Image Correlation,"  
414 *IEEE Trans. Biomed. Eng.*, vol. 66, no. 10, pp. 2740–2752, 2019, doi: 10.1109/tbme.2019.2895283.
- 415

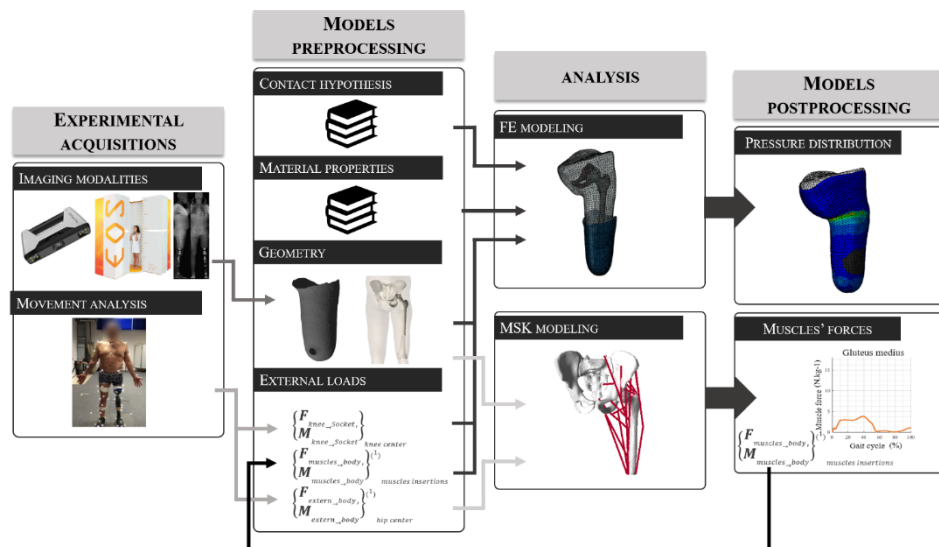
# List of figures

<p>Figure 1</p>	<p>Load distribution applied (Left) to the pelvis segment and considering that ligamental forces may be neglected and (Right) to the prosthetic socket. W: weight of the subject without the residual limb action of the trunk on the pelvis and action of the contralateral limb on the pelvis, T<sub>muscles</sub>: tension forces applied by the muscles inserting on the pelvis, F<sub>femur</sub>: contact force applied by the femur to the pelvis, F<sub>ischial support</sub>: contact force applied by the soft tissues to the pelvis, P: weight of the socket, F<sub>contact</sub>: contact forces applied by the soft tissues to the socket, F<sub>prosthesis</sub>: force applied by the prosthesis to the socket</p> 
<p>Figure 2</p>	<p>3D reconstructions of the femur and pelvis and optical markers (yellow dots) added to the frontal and sagittal EOS radiographs.</p>



Schematic representation of the models design. Experimental acquisitions included using optical scanner, X-rays and kinematic analysis. These data were used with other literature data as input to the MSK and FE models. In particular the MSK model allowed to identify muscles 'forces at 25 % of the gait cycle. These forces were injected into the FE model to compute pressure distribution.

Figure 3



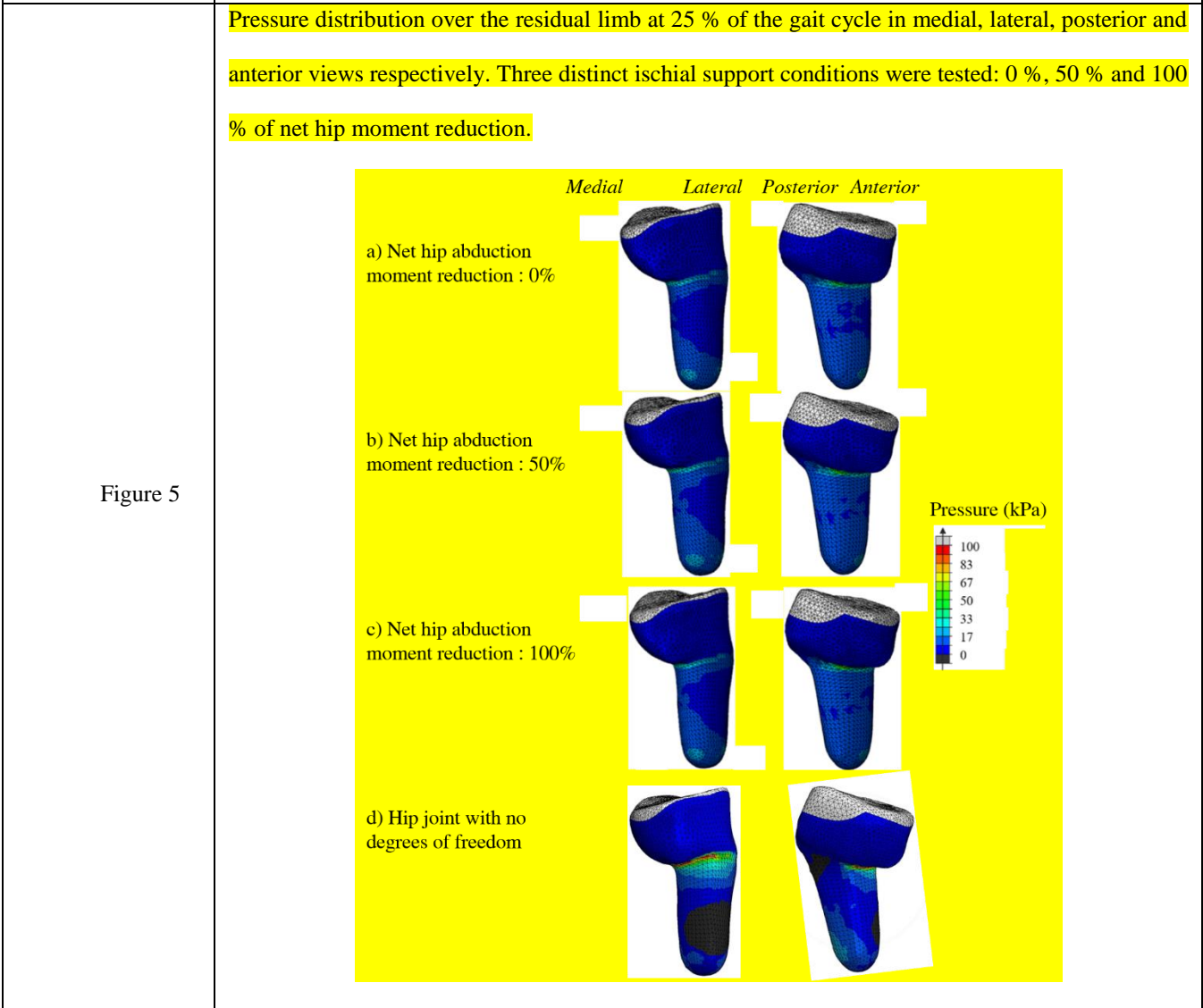
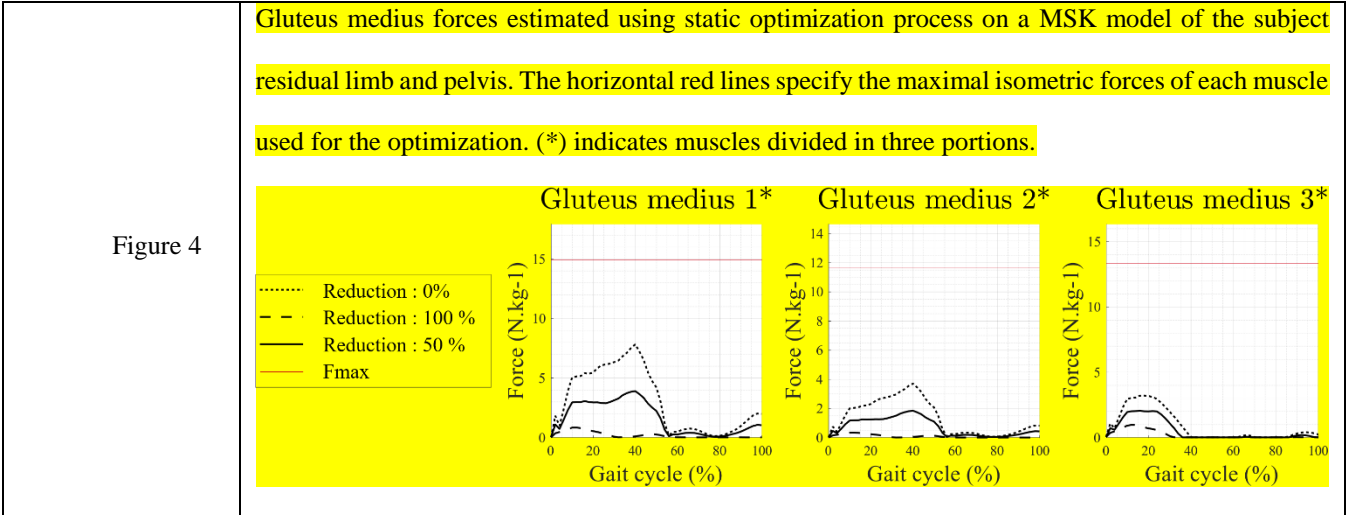


Table 1	Loads expressed at the knee joint center and hip joint center respectively at 25 % of the gait cycle. (*) Loads neglected in this study.		
	Loads	At knee center	At hip center
	$F_{\text{antero-posterior}} \text{ (N)}$	-1	-53
	$F_{\text{vertical}} \text{ (N)}$	622	-515
	$F_{\text{medio-lateral}} \text{ (N)}$	51*	24
	$M_{\text{abduction}} \text{ (N.m)}$	-17*	43
	$M_{\text{external rotation}} \text{ (N.m)}$	-7*	1*
	$M_{\text{Flexion}} \text{ (N.m)}$	27	-19

418